

We are IntechOpen, the world's leading publisher of Open Access books Built by scientists, for scientists

6,900

Open access books available

185,000

International authors and editors

200M

Downloads

Our authors are among the

154

Countries delivered to

TOP 1%

most cited scientists

12.2%

Contributors from top 500 universities



WEB OF SCIENCE™

Selection of our books indexed in the Book Citation Index
in Web of Science™ Core Collection (BKCI)

Interested in publishing with us?
Contact book.department@intechopen.com

Numbers displayed above are based on latest data collected.
For more information visit www.intechopen.com



Diagnostic System in Electrical Impedance Mammography: Background

Alexander Karpov, Andrey Kolobanov and
Marina Korotkova

Additional information is available at the end of the chapter

<http://dx.doi.org/10.5772/intechopen.69195>

Abstract

Electrical impedance mammography (EIM) belongs to nonlocal techniques of image creation. It is based on a number of data collection methods, including the cross-sectional approach, the back-projection method with the weight function applied horizontally and vertically, and the static image method. The analysis of data acquired by applying the above methods enabled to work out the EIM diagnostic system. It involves the following diagnostic categories: structural percentile limits and the mammary gland structure, age-related percentile limits and age-related electric conductivity, outlying values statistics and early diagnostics of breast cancer, D-statistics and distortion of the mammographic scheme in the presence of breast cancer, diagnostic table, and the assessment of the electrical impedance image.

Keywords: electroimpedance mammography, breast cancer, high-risk group

1. Introduction

Modern academic research and clinical practice avail of various tomography systems of electrical impedance diagnostics [1–7]. Electrical impedance mammography (EIM) represents one of the most rapidly developing imaging modalities designed for breast cancer detection [8–22].

EIM belongs to noninvasive techniques of image creation. It measures electromagnetic phenomena and assesses their changes via external scanning.

Since electric current distribution is not limited by two-dimensional plane, the data obtained reflect the change of electric conductivity in three-dimensional space, thus providing for the

layer-by-layer image of the object. Based on the reconstruction of internal distribution from a set of external points, EIM refers to tomography techniques of image construction.

There exist two types of techniques creating tomographic images: local and nonlocal. The local technique implies the passage of one direct ray through the body causing the creation of one pixel in the image. The pixel value depends solely on the substance that the ray meets on its way. X-ray, magnetic resonance, and positron emission all belong to local or hard-field tomography techniques.

The nonlocal technique is characterized by all points on the object affecting the measurement result. This is the so-called cross measurement. The pixel value depends both on the object structure and the structure of the surrounding tissues. Electrical impedance, ultrasound reflection, and optical tomography belong to the category of nonlocal or soft-field tomography techniques.

Thus, EIM is a noninvasive technique featuring nonlocal properties of tomographic image creation.

2. Diagnostics system in electrical impedance mammography

Modern electrical impedance mammography systems, both commercial and experimental, differ in the following characteristics: alternating current parameters, electrode number and arrangement configuration, method of data collection, and algorithm of image reconstruction. Electrical impedance mammograph, MEIKv5.6, developed and manufactured by “PKF “Sim-technika,” Russia was used for the creation of electrical impedance images [22].

The mammograph has the following significant characteristics:

- Noninvasive technology of image creation
- 3D-tomography system
- Form of “soft-field” tomography
- “Nonlocal” method of tomographic image creation
- 50 kHz frequency and 0.5 mA amplitude alternating current
- Planar positioning of electrodes
- 256 electrode panel
- Cross-sectional approach to data collection. The cross-sectional approach is a variation of the complementary method, when all electrodes are involved in measurement pairwise.
- Back-projection method as an algorithm of image reconstruction
- Static image
- Quantitative diagnostic information

The analysis of data obtained via the MEIKv5.6 electrical impedance mammograph allowed to pick out the following diagnostic categories:

- Structural percentile limits and mammary gland structure
- Age-related percentile limits and age-related electric conductivity
- Outlier statistics and early detection of breast cancer
- D-statistics and distorted mammographic scheme in the presence of breast cancer
- Diagnostic table and EIM image evaluation

2.1. Structural percentile limits and mammary gland structure

The analysis in hand is based on data acquired from 1632 electromammographic examinations of normal women of various age groups. It is essential that the test groups contained about the same number of women: 380 women aged 20–30, 428 women aged 31–40, 449 women aged 41–50, and 375 women aged 51–60. The analysis of the electrical impedance mammograms was carried out “blindly”, i.e., without taking the women's age into account.

The fluctuations of the electrical impedance index values made from 0.01 standard units, the lower range value, to 0.68 standard units, the upper range value. To define the structure of electric conductivity index distribution, we extracted eight property ranges with the 0.09 step and calculated the number of observations in each range (**Table 1**).

Figure 1 shows data distribution by the electric conductivity index. The conductivity index mean value constituted 0.29, median, and 0.26, mode.

A bell-shaped curve, similar mean, median, and mode values allow us to declare the quantitative variable (electric conductivity index in this case) distribution as normal. Mean value and

Electric conductivity index	Number of observations
0.05–0.14	0
0.15–0.24	67
0.25–0.34	279
0.35–0.44	471
0.45–0.54	435
0.55–0.64	299
0.65–0.74	75
0.75–0.84	6
Total	1632

Table 1. Distribution of mean electric conductivity index frequencies.

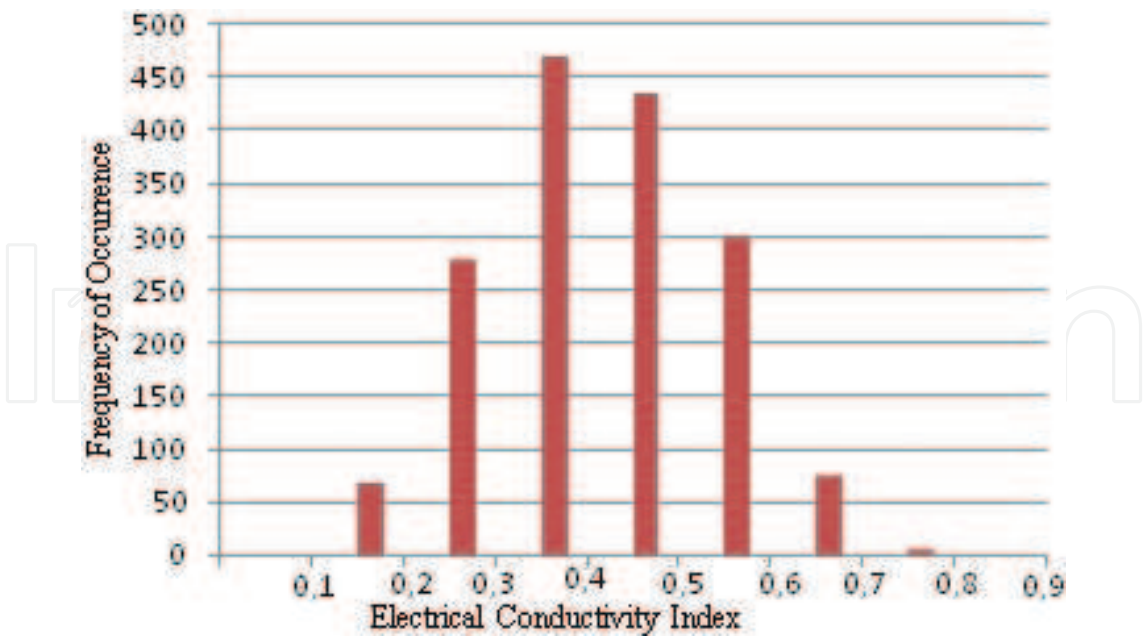


Figure 1. Histogram of mean electric conductivity index frequency distribution.

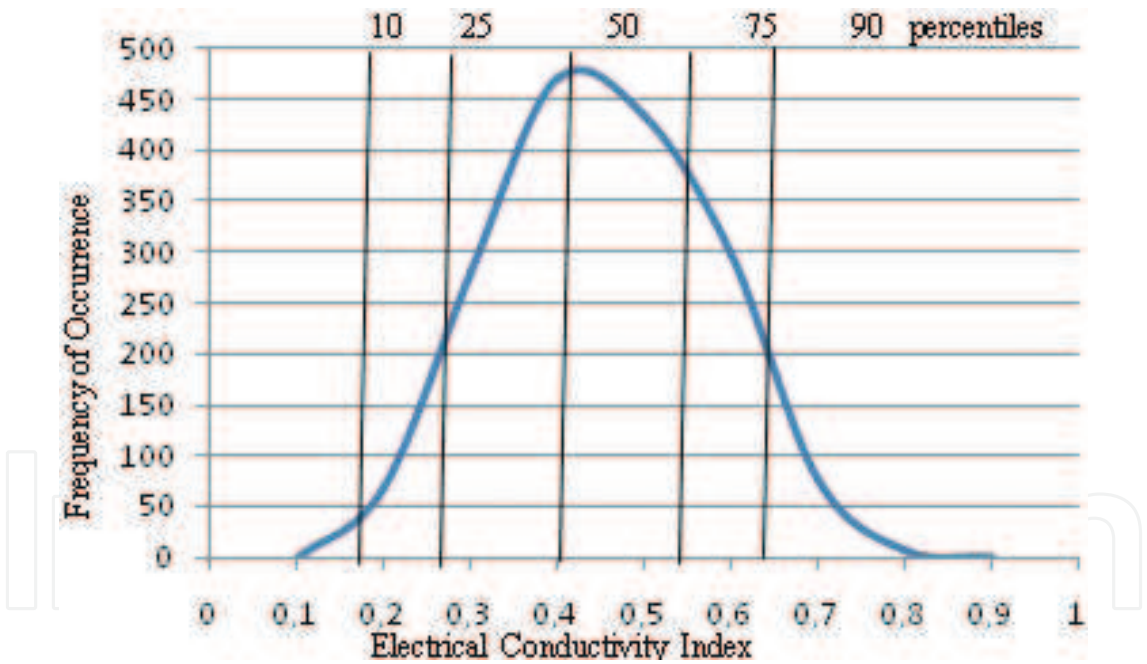


Figure 2. Frequency polygon and percentile ranges.

standard deviation are generally used for normal distribution characterization. We see the implementation of the 10th, 25th, 50th, 75th, and 90th percentile as most rational since it does not require the knowledge of the variable distribution form (Figure 2).

In accordance with the proposed assessments, the values within the first range (below the 10th percentile) should be considered as distinctly low, within the second range (10th–25th percentile) as low, the third and fourth ranges (25th–75th percentile) as mean, within the fifth

range (75th–90th percentile) as high, and the sixth range (above the 90th percentile) as distinctly high.

The mammary gland structure allows to distinguish a few kinds of tissues performing various functions (epithelial, connective, nerve, blood, and lymph). The age involution of the mammary gland consists in the reduction of ductal epithelium proliferation, in the substitution of the secretory epithelium by a connective tissue with different correlations of tissue elements. The electric conductivity index (IC) obtained from the electrical impedance scanning is a quantitative variable, which characterizes the mammary gland structure. A low index is typical of a gland containing a big number of cell elements and thereafter high ion concentration. This causes us to regard the mammary gland structure with the conductivity index percentile limit <10 percentile as representing the ductal type. This is confirmed by the fact that the proportion of the test-group women aged 20–30 with the ductal type of the mammary gland structure and indices fitting in the first channel (<10 percentile) exceeded 70%. A high electric conductivity index is typical of a gland containing big number of fat lobules and a lot of connective tissue and therefore low ion concentration. Thus, the mammary gland structure with the conductivity index percentile limit >90 percentile should be estimated as representing the amorphous type. This is confirmed by the fact that the proportion of women aged 51–60 with the involutive type of the mammary gland structure and indices fitting in the sixth channel (>90 percentile) also exceeded 70%. The mammary gland structure with the conductivity index percentile limit between the 25th and 75th percentile should be estimated as representing the mixed type. This is proved by the fact that this percentile channel included data of women of all age-groups. Different combinations of structures determining tissue electric conductivity produce a wide range of conductivity index values.

Table 2 presents a summary table of the mammary gland structure assessment from the perspective of EIM execution.

Thus, the mammary gland structure can be assessed from the perspective of electrical impedance mammography with a view to the electric conductivity index. As is well-known, the mammary gland structure conditions its density, which is why the distinguished ranges of electric conductivity correspond to different types of breast density. The so-called dense breasts, which correlate with the ductal structural type, are characterized by low values of

Structural type	Electric conductivity	Percentile limits
Amorphous	Above 0.66	>90‰
Mixed with the predominance of the amorphous component	0.57–0.65	75–90‰
Mixed	0.30–0.56	25–75‰
Mixed with the predominance of the ductal component	0.22–0.29	10–25‰
Ductal	Below 0.22	<10‰

Table 2. Types of mammary gland structure from the perspective of electrical impedance mammography.

electric conductivity index. High index values are typical of the amorphous structure when the mammary gland chiefly consists of the adipose and connective tissues. The peculiarity of this approach to the mammary gland structure assessment is a quantitative expression of the mamma's anatomic and histological composition. The results of the mammary gland density assessment from the perspective of electrical impedance mammography with a view to the electric conductivity index are presented in **Table 3**. The assessment is done in line with the American College of Radiology (ACR) terms [23].

2.2. Age-related percentile limits and age-related electric conductivity

The analysis in hand is based on data acquired from over 2000 electromammographic examinations of normal women aged 20–80. The analysis of the electrical impedance mammograms was carried out using the percentile limits approach, the women's age taken into account. It should be noted that modern medical, biological, and clinical research has been increasingly employing the percentile approach as a method of concise description of distributions. This approach does not require the knowledge of distribution form, i.e., it is nonparametric. The use of percentile curves is routine for many diagnostic modalities, e.g., they are widely used for the assessment of fetal development in ultrasound diagnostics. 5, 50, and 95 percentile limits for the electric conductivity index were calculated in each age group, which allowed to draw percentile curves (**Figure 3**) and make a table summarizing percentile limits of normal age-related electric conductivity of the mammary glands (**Table 4**).

Percentile limits of age-related electric conductivity can be used for the formation of breast cancer risk groups. The conductivity index values below the 5th percentile must be regarded as distinctly low, whereas the values exceeding the 95th percentile as distinctly high.

The risk group for breast cancer should thus include patients exhibiting abnormally low age-related electric conductivity values, i.e., below the 5th percentile, which witnesses for extremely high density of the glandular tissue ductal component. High density of the ductal

	<i>EIM classification</i>	Electric conductivity	<i>ACR classification</i>
Type Ia	Amorphous	above 0.66	Predominantly fat, parenchyma below 25%
Type Ib	Mixed with the predominance of the amorphous component	0.57–0.65	
Type II	Mixed	0.30–0.56	Fat with some fibroglandular tissue, parenchyma between 25 and 50%
Type III	Mixed with the predominance of the ductal component, high density of the ductal component	0.22–0.29	Heterogeneously dense, parenchyma 50–75%
Type IV	Ductal, extremely high density of the ductal component	below 0.22	Extremely dense, parenchyma 75–100%

Table 3. Mammary gland structure and density types from the perspective of EIM execution in accordance with the ACR classification.

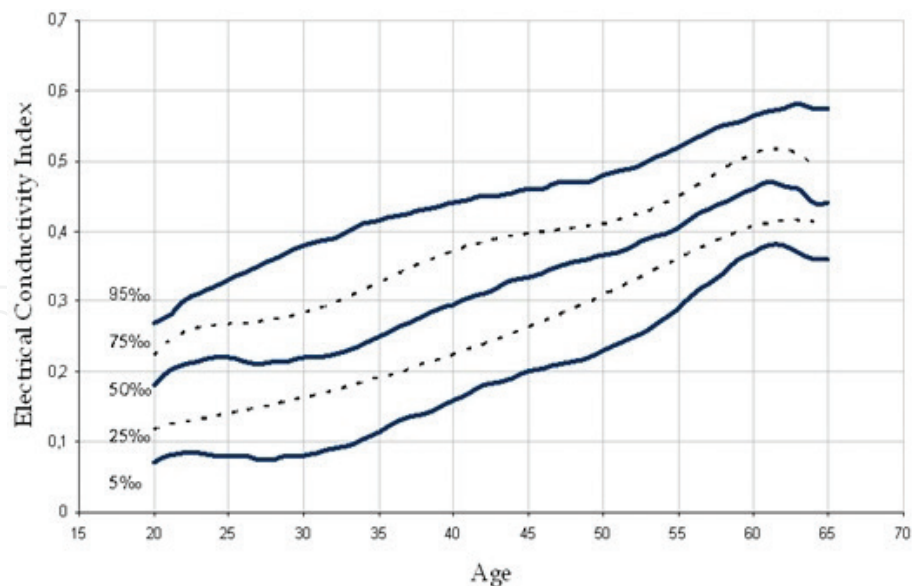


Figure 3. Percentile curves of age-related electric conductivity of the mammary gland.

Age range, years	5 percentile	50 percentile	95 percentile
20–29	0.18	0.28	0.44
30–39	0.16	0.40	0.53
40–49	0.22	0.51	0.63
50–59	0.32	0.58	0.72
60–69	0.43	0.57	0.78
over 70	0.50	0.57	0.64

Table 4. Age-related percentile limits of the mean electric conductivity index.

component carries potential threat since it is often conjoined by the insufficient trophic function of the connective tissue, which is known to be provided by the main substance thereof. Dyscrasia may result in dystrophic processes, including those in the basal membrane.

Abnormally high values of age-related electric conductivity, i.e., exceeding the 95th percentile, correlate with menstrual disorders, the latter standing for hormonal changes.

2.3. Outlier statistics and early detection of breast cancer

Unlike other tomographic modalities which only avail of visual evaluation feature, electrical impedance scanning also provides quantitative information. These unique data are used for diagnostic purposes. A detailed description thereof demands a short reference to outlier statistics.

Provided that all value variations come from a single general population, they are expected to differentiate by virtue of random causes only and stay within the range of $M \pm 2$ standard

deviation. However, we sometimes come across values, which differ dramatically from the rest of the totality. Such values are often referred to as outliers. In this case, checking the values for the presence of outliers is highly desirable. If such a difference is a result of an error or its cause is unknown, the outlier value should be excluded from the assessment. Elimination of values that are “too remote” from the center of a sample is called sample *censoring*.

There are two basic types of methods implemented for outlier elimination [24]:

- (a) Elimination method with the general standard deviation given.
- (b) Elimination method with the general standard square deviation not given.

In the first case, X and standard deviation are calculated with a view to the results obtained from the sample aggregate; in the second case, the sample is stripped of the suspicious results before the calculations are made. Normalized deviate, which serves a nondimensional characteristic of the variable deviation from the arithmetical mean, is one of the criteria used to determine the outliers (1).

$$t = x - M/\sigma \quad (1)$$

where “ t ” is the outlier detection criterion, “ x ” is an outlier, “ M ” is the mean value for a variant group, and “ σ ” is a standard deviation. “ t_{table} ” stands for standard values of the outlier detection criterion, the values are shown in the table. The values of $t_{table} = 2$, $P = 0.95$ are often used for large selections.

The “three sigma” rule applied for the assessment of the measurement results distributed in accordance with the normal law is one of the simplest outlier detection methods. This rule implies the following: if $X_{outlier} - X > 3S_x$, where S_x is an assessment of the standard deviation measurement, the result is hardly probable and may be considered as a miss. The X and S_x values are calculated without regard to the extreme values of $X_{outlier}$.

In this paragraph, we will comment on the results of an electrochemical test of the MEIK v5.6 electrical impedance mammograph. The figure below shows a prototype installation filled with water. The mammograph was used to acquire an electrical impedance scan of the physiological saline solution (**Figure 4A**). The mean electric conductivity index (IC) made 1.85,

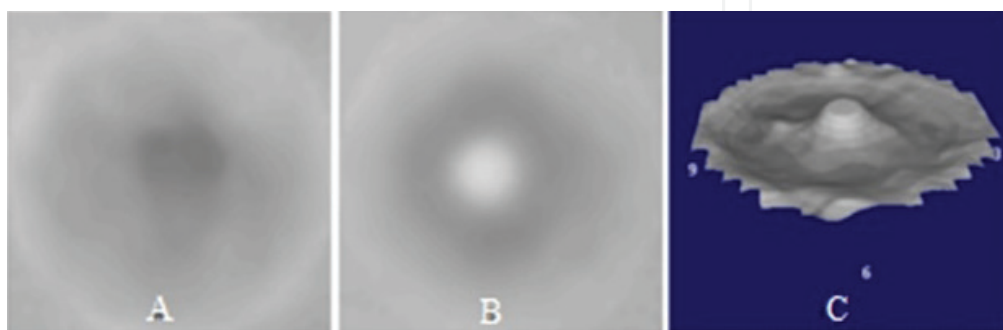


Figure 4. Electroimpedance scans (11 mm deep) of water: A–homogeneous, B–with a metal coin in the middle, C–a 3D image.

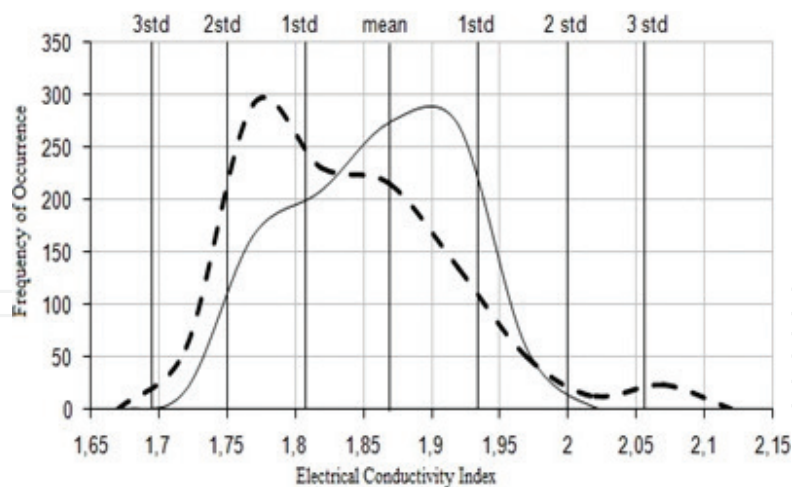


Figure 5. Histograms of electric conductivity distribution of water (continuous curve) and of water with a coin (dotted curve).

whereas the standard deviation amounted to 0.075 and three standard deviations to 0.22. Then, a metal coin was put into the water, 1 cm deeper than the mammograph panel with electrodes (**Figure 4B**). When overlapped, the conductivity distribution histograms (**Figure 5**) allow to see that the IC of the coin (dotted curve) is higher than the IC of water (continuous curve) by a value exceeding three standard deviations. This is typical of outliers; however, in this particular case, it speaks for the presence of an object whose IC value is significantly different from that of the medium, neither does the object belong to the general observation population.

The above mentioned fully applies to medical and biological measurements. **Figure 6** shows an electrical impedance mammogram of a patient suffering from breast cancer, the quantitative parameters being: IC = 0.56, standard deviation=0.12. At 3 o'clock next to the areola, we can see an indistinctly contoured focus with the IC of 0.94. Thus, the IC in the area of interest exceeds the IC of the mammogram by a value going over 3 standard deviations. On the right, we present X-ray and ultrasound images of the same case.

The given example proves that the electric properties of malignant tumors differ significantly from those of the surrounding tissue. It is a well-known fact that cancer cells exhibit an increased electrical activity. Some of the characteristic features of cancer cells that affect their electrical activity are:

1. Cancer cells have cell membranes that exhibit different electrochemical properties and a different distribution of electrical charges than normal tissues [25].
2. A change in mineral content of the cell, particularly an increase in the intracellular concentration of positively charged sodium ions and an increase in the negative charges on the cell coat (glycocalyx) are two of the major factors causing cancer cells to have lower membrane potential than normal cells [25].
3. Cancer cells exhibit both lower electrical membrane potentials and lower electrical impedance than normal cells [26, 27].

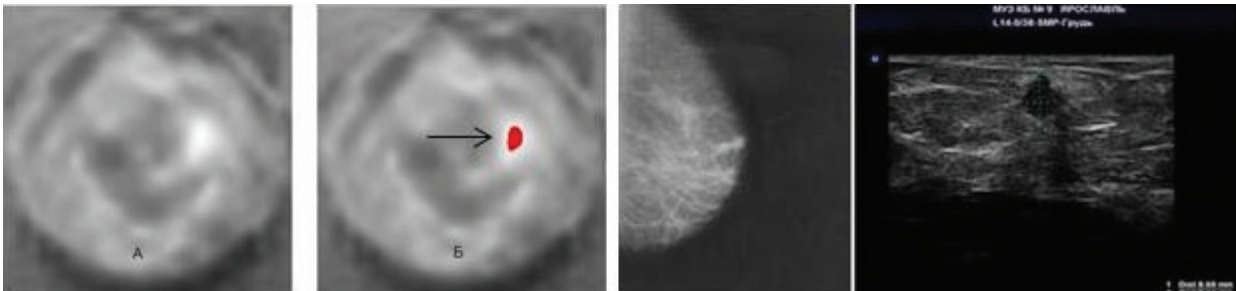


Figure 6. On 3 o'clock next to the areola, a focus is visualized (A), highlighted–arrow (B), less than 10 mm in size. X-ray: A lesion of less than 1 cm in size with a radiant contour in the upper-outer segment. US: a lesion of an irregular shape, 9 × 9 mm without vascularization.

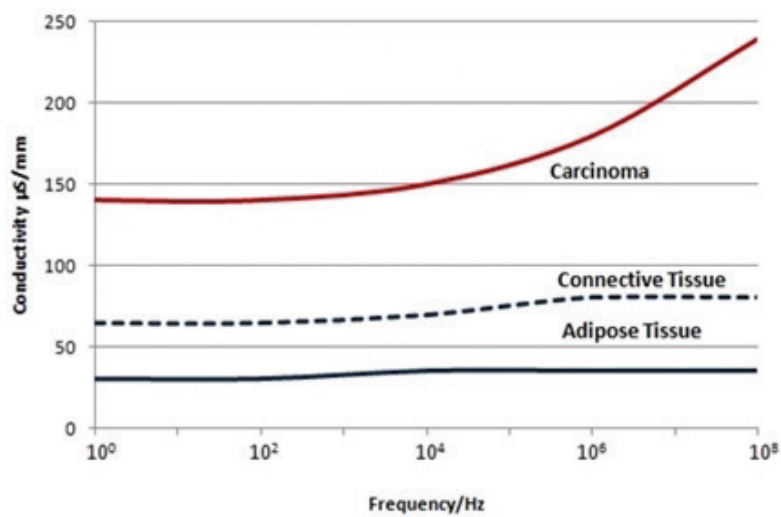


Figure 7. Influence of the current frequency on the electric conductivity of the mammary gland tissues.

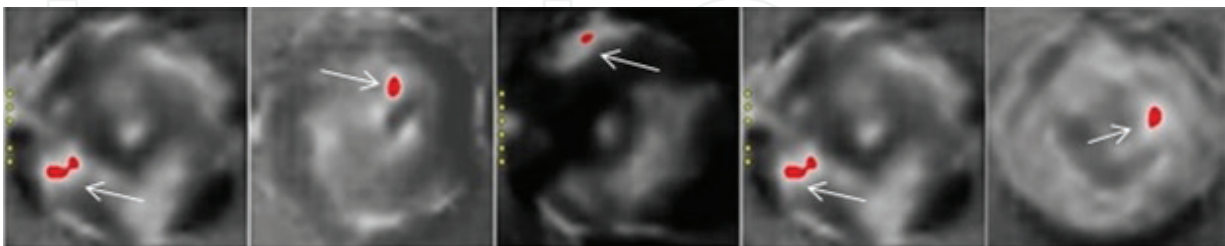


Figure 8. High electrical conductivity area (>3 std) outside the lactiferous sinus zone, which is highlighted (arrow).

From **Figure 7**, it becomes clear that the mammary gland carcinoma has three times higher electric conductivity than the surrounding tissues [28].

This knowledge can be applied to early detection of breast cancer. To perform this task one is to search for areas with abnormal values of $IC > 3 \text{ std}$, which is typical of an oncologic process

with tumors not exceeding 1 cm. To make the search easier, the mammograph highlights abnormal conductivity areas with red (arrow) (**Figure 8**).

2.4. D-statistics and distorted mammographic scheme in the presence of breast cancer

As the disease connected by the breakup of the epithelium basal membrane progresses, various phenomena can occur in the tumor and the surrounding tissues. These processes are always accompanied by alterations of electrical properties of the tumor mass. Increased vascularization leads to electrical conductivity increase due to ionic conduction. Replacement of dead tumor cells by collagen fibers leads to electrical conductivity decrease. While purulent inflammation areas emerge, permittivity decreases as a result of the cell membranes death. Lymphocytic infiltration causes the tumor and the surrounding tissues impedance to increase, because of a significant local concentration of cell membranes. Thus, tumor growth is regularly accompanied by the alteration of the electrical properties both of the tumor and the surrounding tissues.

As noted previously, the electrical impedance approach enables to conduct a quantitative analysis of the image involving the assessment of the following parameters: mean electric conductivity index, histogram of electric conductivity distribution, comparison of the electric conductivity distribution histogram with the referent values.

To refer the patient to the norm or pathology category, the divergence in the distribution form criterion, also known as the λ -criterion or the Kolmogorov-Smirnov criterion [29], is used in Eq. (2).

$$\lambda = \left| \sum N1(xij)/n1 - \sum N2(xij)/n2 \right| \max \sqrt{n1n2/n1 + n2} \quad (2)$$

where $N1$ stands for observation quantities within the ranges, $n1$ —within the sample aggregate, A_1 ; and $N2$ and $n2$ —the same for A_2 .

Dx statistics, to be more exact, a subaggregate when calculating the Kolmogorov-Smirnov criterion Eq. (3).

$$D(xij) = \left| \sum N1(xij)/n1 - \sum N2(xij)/n2 \right| \max \quad (3)$$

where $N1$ stands for observation quantities within the ranges, $n1$ —within the sample aggregate, A_1 ; $N2$ and $n2$ —the same for A_2 .

This nonparametric criterion enables to determine the statistical significance of divergences in the distribution of any characteristic of norm or pathology including the distribution of electric conductivity on electrical impedance tomograms.

The Dx statistics allows to define the area of one of the distributions, which is not shared by the other (**Figure 9**). The Dx value reflects the proportion of observations or data, which distinguishes experiment (patient) from control (norm). This value is essential for substantiation of diagnosis as well as for assessing the parameter information capacity.

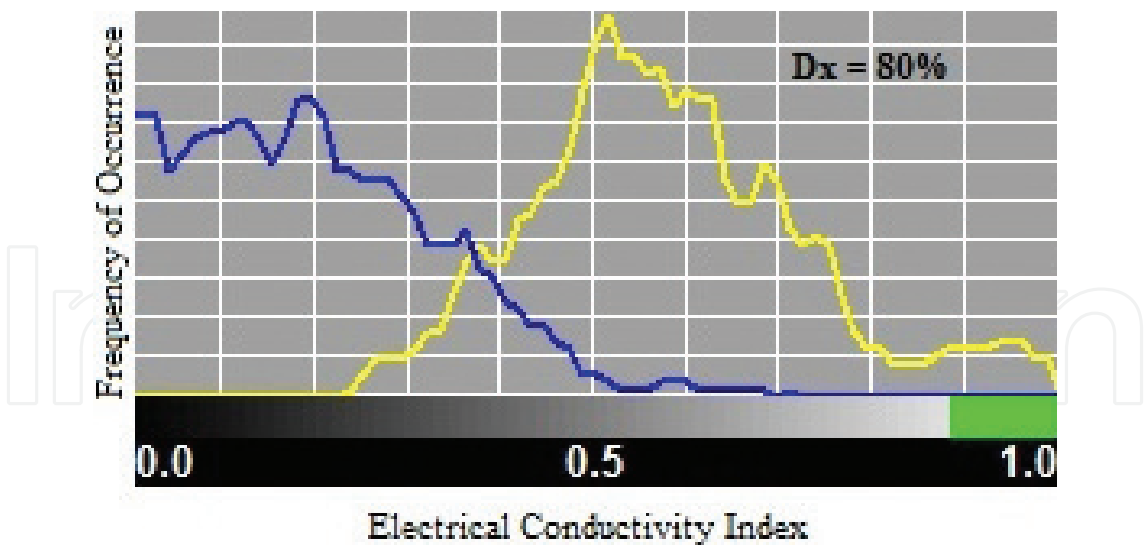


Figure 9. Assessment of distribution divergence by their area.

High information capacity of the divergences revealed enables to refer the patient to this or that category (e.g., norm or cancer) with great probability. To determine the informative value of distribution divergence Kulback's information measure is applied Eq. (4).

$$J = 10 \lg P1/P2 * 0.5(P1 - P2) \tag{4}$$

where *J* = information value of the range, *P1*–probability of patients' suffering from disease A1 getting into the range, *P2*–the same for disease A2.

It shows how informative the Dx statistics applied is, how this parameter contributes to diagnosing the disease, e.g., cancer. The assessment of distribution divergence (Dx) produced results standing in direct relationship with the information capacity, according to Kulback (Table 5). This relationship must be recognized as fairly regular and consistent [29].

In the presence of cancer, the histogram of the affected gland is shifted. Table 6 sums up data on comparative electric conductivity obtained from patients suffering breast cancer, benign changes of the mammary gland as well as from normal women with different types of mammary gland structure.

In the course of oncologic process development, general and local electric conductivity naturally tends to change. The distortion of the mammographic scheme can be observed as early

Distribution divergence	Information capacity	Reliability
below 20%	Very low	No
20–30%	Relatively low	Yes
30–50%	Good	Yes
50–65%	High	Yes

Table 5. Distribution divergence and information capacity.

	Number of patients	Comparative electric conductivity (affected–normal gland)					
		<20%	20–30%	30–40%	40–50%	50–60%	>60%
Cancer	310	101 (33%)	67 (22%)	44 (14%)	37 (12%)	26 (8%)	35 (11%)
Healthy	161	157 (98%)	4 (2%)	0	0	0	0
Healthy acinar-ductal type	20	18 (90%)	1 (5%)	1 (5%)	0	0	0
Healthy amorphous type	32	28 (88%)	2 (6%)	2 (6%)	0	0	0
Benign	68	59 (87%)	7 (10%)	2 (3%)	0	0	0

Table 6. Comparative electric conductivity of the mammary glands, data acquired from patients suffering from breast cancer, benign lesions, and normal women.

Diagnostic criteria	Electrical impedance mammography points
<i>Shape</i>	
• Round, oval	1
• Lobular, irregular	2
<i>Contour</i>	
• No	0
• Sharp	1
• Hyperimpedance, indistinct	2
<i>Surrounding tissues</i>	
• Preserved	0
• Structure alteration/displacement	1
• Thickening/extrusion/retraction	2
<i>Internal electrical structure</i>	
• Hyperimpedance ($IC_{roi} < IC_{av} - 2std$)	0
• Isoimpedance ($IC_{roi} = IC_{av} \pm 2std$)	1
• Hypoimpedance ($IC_{roi} > IC_{av} + 2std$)	2
• Animpedance ($IC_{roi} > IC_{av} + 3std$)	3
<i>Comparative electrical conductivity</i>	
• Divergence between the histograms <20%	0
• Divergence between the histograms 20–30%	1
• Divergence between the histograms 30–40%	2
• Divergence between the histograms >40%	3

Table 7. Diagnostic criteria for differentiation of volumetric lesions in electroimpedance mammography.

as at onset of the disease that is why this criterion was added to the EIM breast cancer diagnostic scale (Table 7). Below (Figure 10), we provide examples of the distorted mammographic scheme from three patients with breast cancer.

2.5. Diagnostic table and EIM image assessment

A volumetric lesion is an extensional involvement detected on several scan planes. Image analysis implies the assessment of the lesion shape, contour, internal electric structure, and changes in the surrounding tissues.

A diagnostic table was made to regularize the description of volumetric lesions. Table 7 presents assessment parameters each being given a certain set of points.

Using the numerical score for the assessment of volumetric lesions in electrical impedance mammography allows to compare this information to BI-RADS ACR categories (Table 8).

The EIM point scale enables to standardize the description of volumetric lesions when carrying out electrical impedance mammography examination as well as use the algorithm of patients' supervision worked out by the specialists of the American College of Radiology.

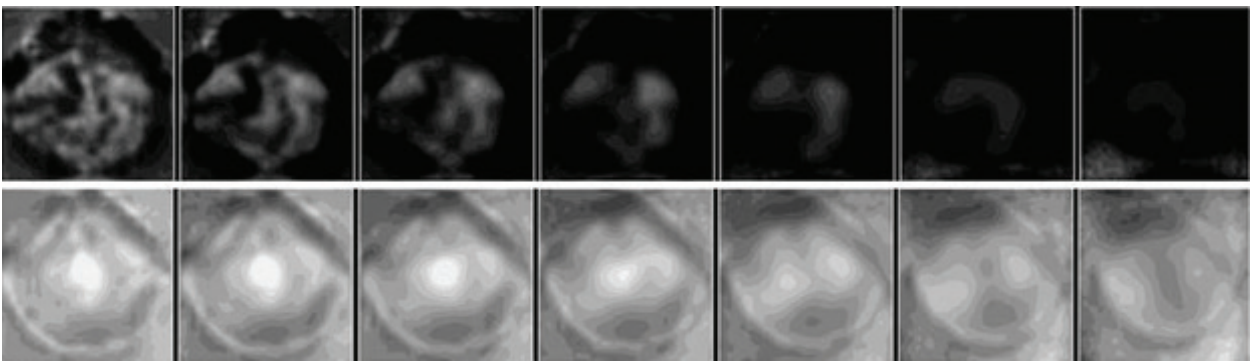


Figure 10. Electroimpedance mammographic scheme distortion (the top images show the affected gland, the bottom line contains images of the normal breast).

EIM	ACR
<i>Common scale</i>	<i>BI-RADS categories</i>
No score	BI-RADS 0 poor image
0–1	BI-RADS 1 lesion is not defined
2–3	BI-RADS 2 benign tumors–routine mammography
4	BI-RADS 3 probably benign findings
5–7	BI-RADS 4 suspicious abnormality–biopsy
>8	BI-RADS 5 highly suggestive of malignancy–treatment/biopsy

Table 8. EIM scale and ACR BI-RADS.

3. Conclusion

EIM diagnostic system is a clear and logical system involving determination of the mammary gland structure and density, allowing for cancer diagnostics for various types of breast as well as formation of breast cancer risk groups.

Author details

Alexander Karpov*, Andrey Kolobanov and Marina Korotkova

*Address all correspondence to: karpovay@medyar.ru

Clinical Hospital, Yaroslavl, Russia

References

- [1] Barber DC, Brown BH. Applied potential tomography. *Journal of Physics E-Scientific Instruments*. 1984;**17**(9):723-733
- [2] Brown BH, Seagar AD. The Sheffield data collection system. *Clinical Physics and Physiological Measurement*. 1987;**8**(Suppl A):91-97
- [3] Electrical impedance tomography. Edited by D.S.Holder, IOP. 2005
- [4] Karpov A, Korotkova M, et al. Electrical impedance potential mammography for visualization of objects (Electrochemical tests). *Journal of Physics: Conference Series*. 2010;**224**:012032
- [5] Akhtari-Zavare M, Latiff L. Electrical impedance tomography as a primary screening technique for breast cancer detection. *Asian Pacific Journal of Cancer Prevention*. 2015;**16**(14):5595-5597
- [6] Shetiye P, Ghatol A, et al. Detection of breast cancer using electrical impedance and RBF neural network. *International Journal of Information and Electronics Engineering*. 2015;**5**(5):P356-360
- [7] Prasad NS, Houserkova D, Campbell J. Breast imaging using 3D electrical impedance tomography. *Biomedical Papers of the Medical Faculty of the University of Palacky, Olomouc Czechoslovakia*. 2008;**152**(1):151-154
- [8] Cherepenin V, Karpov A, Korjnevsky A, Kornienko V, Mazaletskaya A, Mazurov D, Meister D. A 3D electrical impedance tomography (EIT) system for breast cancer detection. *Physiological Measurement*. 2001;**22**:9-18
- [9] Cherepenin V, Karpov A, Korjnevsky A, Kornienko V, Kultiasov Y., Ochapkin M, Trochanova O, Meister J. Three-dimensional EIT imaging of breast tissues: System design and clinical testing. *Medical Imaging*. 2002;**V21N6**:662-667

- [10] Karpov A, Korjenevsky A, Mazurov D, Mazaletskaya A. 3D electrical impedance scanning of breast cancer. World Congress on Medical Physics and Biomedical Engineering, Chicago; 2000; p. 62
- [11] Halter RJ, Hartov A, Paulsen KD. A broadband high-frequency electrical impedance tomography system for breast imaging. *IEEE Transactions on Biomedical Engineering*. 2008;**55**(2 Pt 1):650-659
- [12] Jossinet J. A hardware design for imaging the electrical impedance of the breast. *Clinical Physics and Physiological Measurement*. 1988;**9**Suppl A:25-28
- [13] Kerner TE, Paulsen KD, Hartov A, Soho SK, Poplack SP. Electrical impedance spectroscopy of the breast: Clinical imaging results in 26 subjects. *IEEE Transactions on Medical Imaging*. 2002;**21**(6):77-80, 95-100
- [14] Kim, BS, Boverman, G, Newell, JC, Saulnier, GJ, Isaacson, D. The complete electrode model for EIT in a mammography geometry. *Physiological Measurement*. 2007;**28**(7):S57-S69
- [15] Raneta O., Ondruš D., Bella V. Utilisation of electrical impedance tomography in breast cancer diagnosis. *Klinická Onkologie*. 2012;**25**(1):36-41
- [16] Karpov A, Korotkova M. Diagnostic criteria for mass lesions differentiating in electrical impedance mammography. *Journal of Physics: Conference Series*. 2013;**434**:012053
- [17] Chakraborti K, Selvamurthy W. Clinical application of electrical impedance tomography in the present health scenario of India. *Journal of Physics: Conference Series*. 2010;**224**:012069
- [18] Zain N., Kanaga K. A review on breast electrical impedance tomography clinical accuracy. *ARPN Journal of Engineering and Applied Sciences*. v2015;**10**(15):P6230-6234
- [19] Pak D, Rozkova N, et al. The electroimpedance computer tomography in screening of diseases of the breast. *Medical Visualization*. 2012;**2**:P35-42
- [20] Zain N, Chelliah K. Breast imaging using electrical impedance tomography: Correlation of quantitative assessment with visual interpretation. *Asian Pacific Journal of Cancer Prevention*. 2014;**15**(3):1327-1331
- [21] Korotkova M, Karpov A, et al. Electrical impedance imaging characteristics of nodular and edematous-infiltrative forms of breast cancer. *Breast Cancer Symposium*. San Antonio. 2011:6-10
- [22] Korotkova M, Karpov A. Standards for Electrical Impedance Mammography In book "Imaging of the Breast. Technical Aspects and Clinical Implication". Edited by Tabar L, Croatia, 2014
- [23] Breast Imaging Reporting and Data System (BI-RADS). 4th ed. Reston: American College of Radiology; 2003
- [24] Zaydel A. Error of Measurement of Physical Quantities. 1985
- [25] Cure JC. On the electrical characteristics of cancer. Paper presented at the Second International Congress of Electrochemical Treatment of Cancer. 1995; Florida

- [26] Cone CD. Variation of the transmembrane potential level as a basic mechanism of mitosis control. *Oncology*. 1970;**24**:438-470
- [27] Blad B, Baldetorp B. Impedance spectra of tumour tissue in comparison with normal tissue: A possible clinical application for electrical impedance tomography. *Physiological Measurement*. 1996;**17**Suppl 4A:A105-A115
- [28] Jossinet J. The impedivity of freshly excised human breast tissue. *Physiological Measurement*. 1998;**19**:61-75
- [29] Gubler E. Quantitative methods for analysis and identification of pathology. Leningrad. 1978

